Chapter 9
Slope Instability of Glaciated Continental Margins: Constraints from Permeability-Compressibility Tests and Hydrogeological Modeling Off Storfjorden, NW Barents Sea

J. Llopart, R. Urgeles, A. Camerlenghi, R.G. Lucchi, B. De Mol, M. Rebesco, and M.T. Pedrosa

Abstract Climate variations control sediment supply to the continental slope as well as glacial advances and retreats, which (a) cause significant stress changes in the sedimentary column and redistribution of interstitial fluids, (b) induce a particular margin stratigraphic pattern and permeability architecture and (c) are at the origin of isostatic adjustments that may reactivate faults. We test this hypothesis using a combination of geophysical and geotechnical data from the Storfjorden Trough Mouth Fan, off southern Svalbard. The results of compressibility and permeability testing are used together with margin stratigraphic models obtained from seismic reflection data, as input for numerical finite elements models to understand focusing of interstitial fluids in glaciated continental margins and influence on timing and location of submarine slope failure. Available results indicate values of overpressure of 0.23–0.5 (slope-shelf) that persist to present-day. This overpressure started to develop in response to onset of Pleistocene glaciations and reduced by half the factor of safety of the continental slope.

Keywords Overpressure • Hydrogeology • Factor of safety • Storfjorden • Barents Sea • Hydrogeologic model

J. Llopart (✉) • B. De Mol • R. Urgeles
Dept. Geociències Marines, Institut de Ciències del Mar (CSIC), Barcelona, Spain
e-mail: jaume.llopart@gmail.com

A. Camerlenghi • R.G. Lucchi • M. Rebesco
Geophysics Research Section, Istituto Nazionale di Oceanografia e Geofisica Sperimentale-OGS, Trieste, Italy

M.T. Pedrosa
Instituto Andaluz de Ciencias de la Tierra-IACT, Granada, Spain

S. Krastel et al. (eds.), *Submarine Mass Movements and Their Consequences*, Advances in Natural and Technological Hazards Research 37, DOI 10.1007/978-3-319-00972-8_9,

9.1 Introduction

During the last decades large submarine landslides have been widely discovered in Polar Regions. The Norwegian margin has been subject of a comprehensive study motivated by the occurrence of gas and oil fields associated to nearby landslides. Large and medium-size landslides are well documented (i.e. the Trænadjupet Slide and the Andøya Slide), including the largest known submarine landslide, the Storegga Slide with a volume of 5600 km^3 (Haflidason et al. 2005; Laberg et al. 2000; Laberg et al. 2002). The thick deposits accumulated during glacial and interglacial cycles have been subject to ice sheet dynamics, loading and unloading by the grounded ice sheet, glacio-eustatic sea-level variations, glacio-isostatic rebound and associated seismicity (Bugge et al. 1987; Mulder and Moran 1995). Continental margin development must have played a significant role in controlling the migration of interstitial fluids, determining the occurrence of sediment instability when combined with depositional oversteeping (Dimakis et al. 2000). The aim of this study is therefore to: (1) characterize the compression and permeability characteristics of glacial-deglacial-interglacial marine sediments of a polar continental margin; (2) reconstruct the paleohydrogeological evolution; and (3) determine how continental margin architecture and physical properties couple to control the location of submarine slope instability.

The study area (Fig. 9.1) is located in the Storfjorden Trough Mouth Fan (TMF) south of the Svalbard archipelago. This TMF covers an area of about 40.000 km^2 and has a radius of about 190 km, developed concentrically off the Storfjorden trough.

9.2 Data and Methods

Consolidation and permeability tests were performed using a GDS Rowe & Barden-type Consolidation cell equipped with three 2 MPa advanced pressure/volume controllers. Atterberg limit were also determined. The liquid limit was determined using an 80 g, 60° apex fall cone device, while the plastic limit was estimated from the hand rolled thin thread of sediment method (Karlsson et al. 1977).

The stratigraphy and 2D architecture of the different units used to perform the hydrogeological modeling correspond to the seismic units defined in between seismic reflections R1-R7 described in Faleide et al. 1996. These seismic reflections were picked on seismic line ITEG08-09 acquired during the Italian cruise EGLACOM (Fig. 9.2). The R7 and the OB (top of Oceanic Basement) reflectors correspond to the projected position of these reflectors on line ITEG08-09 made from the two seismic lines north and south of Storfjorden included in Faleide et al. (1996) as the line ITEG08-09 did not have enough penetration to image these reflectors. The velocities for the time to depth conversion have been approximated from ODP Leg 162 holes 986C and 986D sonic data.

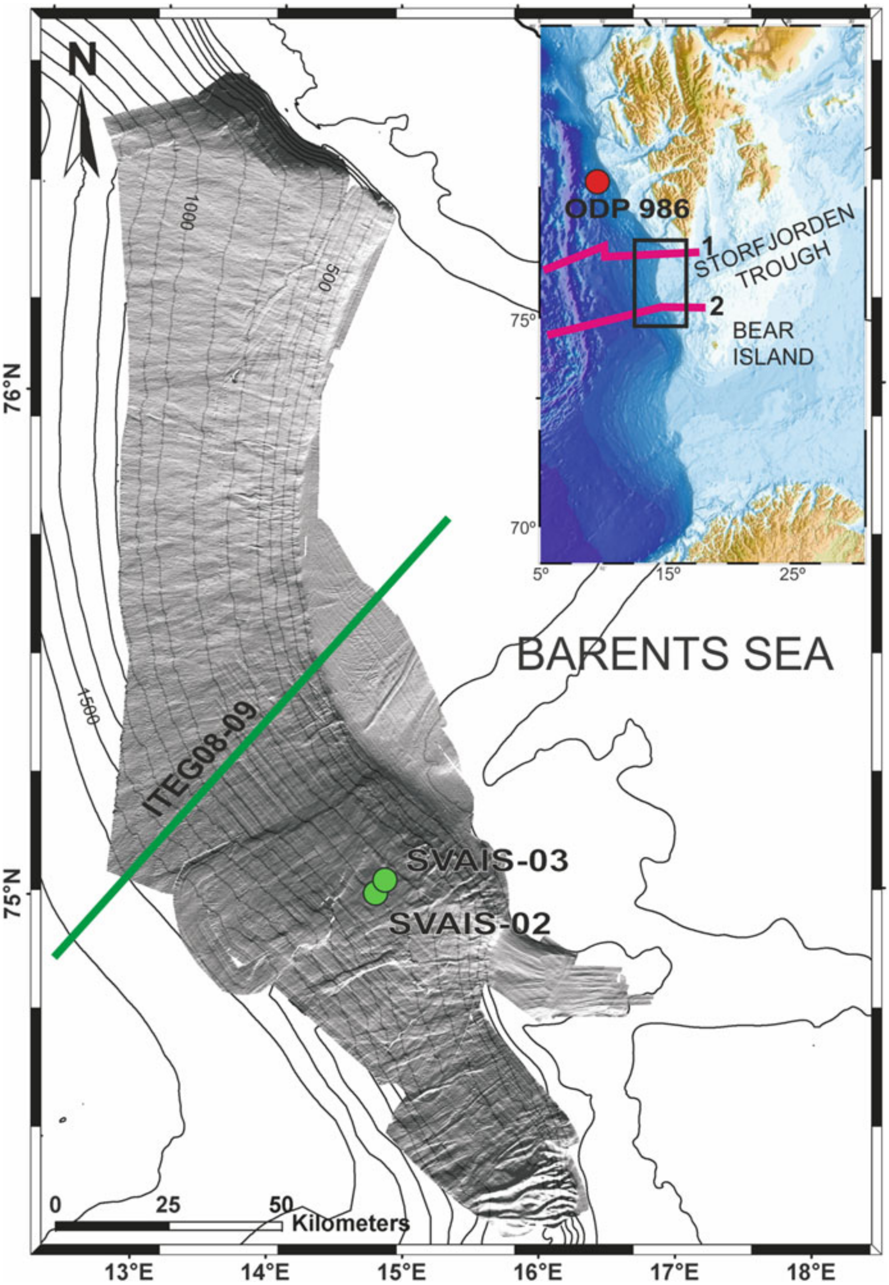

Fig. 9.1 Location of the study area. Bathymetric *shaded* relief showing submarine landslides beyond the shelf break. Seismic lines 1 and 2 (in *pink*) extracted from Faleide et al. 1996 [6] and ITEG08-09 (in *green*) from EGLACOM cruise report (REL OGS 2008/111). *Green dots* are gravity cores. *Red dot* is the Site ODP 986

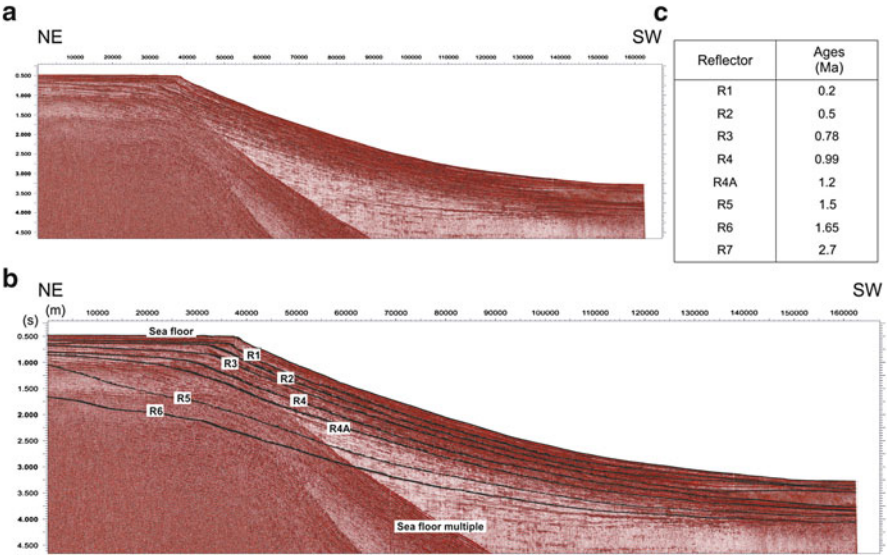

Reflector	Ages (Ma)
R1	0.2
R2	0.5
R3	0.78
R4	0.99
R4A	1.2
R5	1.5
R6	1.65
R7	2.7

Fig. 9.2 (**a**) uninterpreted and (**b**) interpreted EGLACOM ITEG08-09 seismic line used for "BASIN" modelling. (**c**) ages for seismic reflectors [11]

Using the Finite Element Software "BASIN" (Bitzer 1996; 1999) continental margin hydrogeological modelling has been carried out to simulate the fluid migration and pore pressure development. In this study pore pressure is also described in terms of overpressure (λ), defined as (Flemings et al. 2008):

$$\lambda = (P - P_h)/(\sigma_v - P_h) \tag{9.1}$$

where P is pore pressure, P_h is the hydrostatic pressure and σ_v is lithostatic or total stress. The initial thickness (H_i) of different strata used as input for the model was calculated using van Hinte's decompaction equation (Van Hinte 1978):

$$H_i = H_f\,[(1 - \phi_f)/(1 - \phi_i)] \tag{9.2}$$

where ϕ_i is the initial porosity, ϕ_f is the present-day porosity and H_f is the present sediment thickness.

The total length of the modeled transect is around 162 km and the mesh nodes are equally spaced every 4 km. Ice-induced stresses or erosion by ice have not been considered. Sedimentary facies are often represented by a mixture of sediment types, whose composition will vary according to the relative abundance of each sediment type for a given area and unit. Physical properties are also averaged according to the sediment mixture. Time intervals were extracted from Knies et al. (2009) (Fig. 9.2c).

9.3 Results

Consolidation and permeability testing were performed on two sediment types: laminated sediments interpreted as plumites, and glacigenic debris flows (GDFs) (Table 9.1). Pre-consolidation pressures indicate normally consolidated sediments for plumites and GDFs (Table 9.1). Plumites also have higher initial hydraulic conductivity (4.8×10^{-8} m/s compared to 2.9×10^{-8} m/s) and compressibility (0.36 versus 0.19) than GDFs. The specific storage and permeabilities show also a more marked decrease with increasing stress for plumites than for GDFs (Table 9.1 and Fig. 9.3). Geotechnical tests (Fig. 9.3) show that climatically controlled sedimentation changes on polar continental margins produce sediments with contrasting physical properties. The steeper trend in the virgin consolidation and theoretical permeability

Table 9.1 Most important parameters derived from geotechnical tests in this study

	Sediment type	Wi (%)	e_0	k_0 (m^2)	S_0 (m^{-1})	σ_c
SVAIS-02-02	Plumites	44.16	1.804	$5.97E^{-15}$	0.06742	36
SVAIS-02-03	Plumites	42.02	1.894	$5.53E^{-16}$	0.04019	52
SVAIS-02-04	Plumites	39.89	1.729	$5.57E^{-15}$	0.03773	61
SVAIS-02-05	GDF	26.63	1.110	$2.49E^{-15}$	0.01334	67
SVAIS-02-06	GDF	23.14	0.899	$3.31E^{-15}$	0.03003	69
SVAIS-03-06	Plumites	47.86	1.854	$6.85E^{-15}$	0.0327	64

GDF Glacigenic Debris Flows, *Wi* initial water content, e_0 initial void ratio, k_0 initial permeability, S_0 initial specific storage, σ_c pre-consolidation pressure

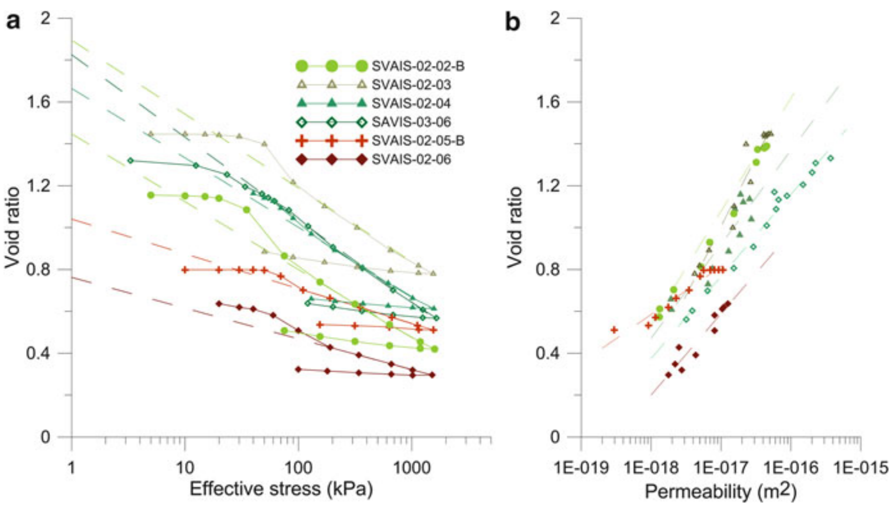

Fig. 9.3 Consolidation tests: (**a**) effective stress/void ratio relationship for the tested samples. (**b**) Flow-through permeability versus void ratio. Extrapolation to 1 kPa is used to determine initial parameters for the simulation. Greenish lines correspond to plumites and reddish to GDFs

Table 9.2 Parameters used for "BASIN" and fluid flow modeling

	Plumites	GDFs	Till	Hemipelagic sediments
Initial porosity	0.64[a]	0.5[a]	0.4[b]	0.778[c]
Grain density (kg/m^3)	2650	2650	2650	2650
Init. Specific storage (m^{-1})	0.025[a]	0.015[a]	0.0056[b]	0.044[c]
Init. hydraulic conductivity (m/s)	4.8E^{-8a}	2.9E^{-8a}	5.3E^{-11b}	3.0E^{-9d}

[a]This study, [b]Shaver (1998), [c]ODP sites 986C/D data, [d]Urgeles et al. (2010)

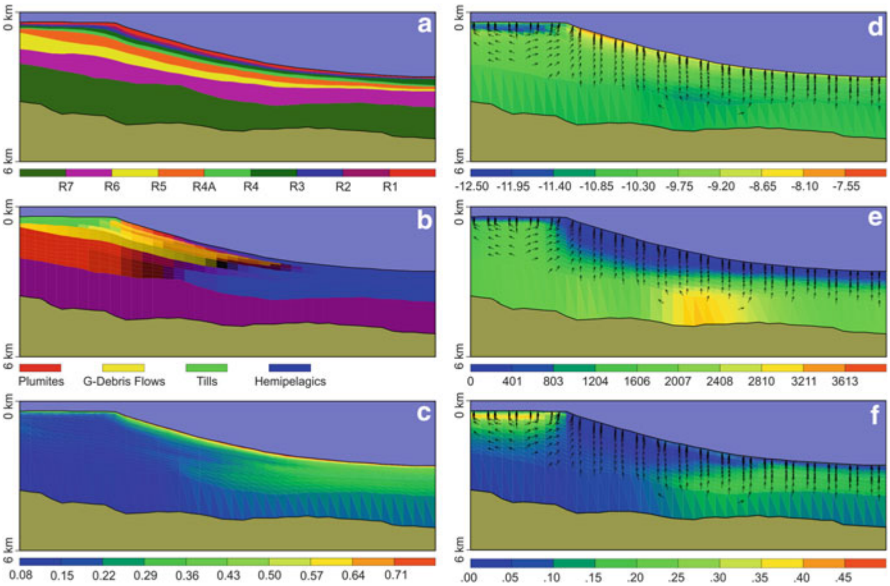

Fig. 9.4 Margin stratigraphic and hydrodynamic modeling with "BASIN" at final simulated present condition. (**a**) Margin stratigraphy according to seismic units described by Faleide et al. (1996). (**b**) Facies composition. (**c**) Fractional porosity. (**d**) Log hydraulic conductivity. (**e**) Excess pore pressure (kPa). (**f**) Overpressure (λ)

lines of plumites clearly highlights these differences (Fig. 9.3). Tests performed on split plumites cores SVAIS-02 and SVAIS-03 indicate higher water content and lower shear strength than the GDFs for a similar burial depth (Lucchi et al. 2012).

The parameters obtained from consolidation/permeability testing (see Table 9.2) have been used as input for the hydrogeological modeling. The last output stage in terms of physical properties and sedimentological/architectural characteristics from the model are presented in Fig. 9.4. At the end of the simulation (present day), the minimum porosities are around 10 % in the continental shelf and upper slope, mainly corresponding to the units consisting of tills and glacigenic debris flows. Hydraulic conductivities for these units have values between 10^{-12} and 10^{-10} m/s, but the values start decreasing at ~1.2 Ma. Overpressure reaches values of ~0.15 near the shelf break and upper slope where the sediment thickness is maximum.

A sensitivity analysis showed that hydraulic conductivity is the parameter that has larger influence on the resulting overpressure than other the parameters involved in the calculations as porosity or specific storage.

9.4 Discussion

"BASIN" modeling allows us to investigate how physical properties, sedimentology and stratigraphic architecture couple to control margin hydrogeology and fluid flow pathways. The simulation shows that low porosities (10–30 %) develop in most of the continental margin, specially the continental shelf and upper-middle slope, due to consolidation and the initial low porosity of till and glacigenic debris flow sediments.

Accumulation of GDFs on the upper-middle continental slope, which has low initial permeability and compressibility, determines the formation of fluid flow divergence beneath the continental shelf and lower slope. Most of the margin shows vertical fluid flow which is a normal situation for a fluid flow trend in a continental margin dominated by consolidation processes. The low porosity and permeability of the tills act as an impervious boundary which results in shallow moderate pore pressure and high overpressure. A more marked reduction in permeability of hemipelagic sediments due to their higher compressibility induces high pore pressures at depth but only moderate overpressure.

Onset of glaciation between 1.8 and 1.6 Ma (Butt et al. 2000; Laberg et al. 2010) provides abundant glacigenic sediments (tills and GDFs) to the continental shelf and upper slope, particularly since intensification of glaciation from 0.99 Ma (~R4) (Knies et al. 2009). These sediments control to a large extent overpressure development. A maximum value of 0.5 is reached on the continental shelf, while the shelf edge and upper slope (where most of the landslides occur in that area) display a lower maximum value of 0.15.

High overpressure in glaciated continental margins may favor onset of slope failure (Kvalstad et al. 2005) and recent and buried landslides have also been identified off Storfjorden (Fig. 9.1) (Lucchi et al. 2012; Rebesco et al. 2012). A preliminary analysis of the factor of safety (FoS) using Eq. (9.3) (Flemings et al. 2008):

$$FoS = \frac{\tan \phi_f}{\sin \phi \cdot \cos \phi} \left(\cos^2 \phi - \lambda \right) \tag{9.3}$$

where ϕ_f is the friction angle (set constant at 28º) and ϕ the slope, shows that overpressure significantly reduced the FoS (FoS > 1 stable and FoS < 1 unstable), but not enough to induce slope failure. Along the reflector R2 (0.5 Ma) (where the largest slope failure is rooted), the steepening during margin development induced a slight decrease of the FoS in the upper slope since its deposition to present day, but an increase in some areas of the lower slope (Fig. 9.5). Close to the seafloor

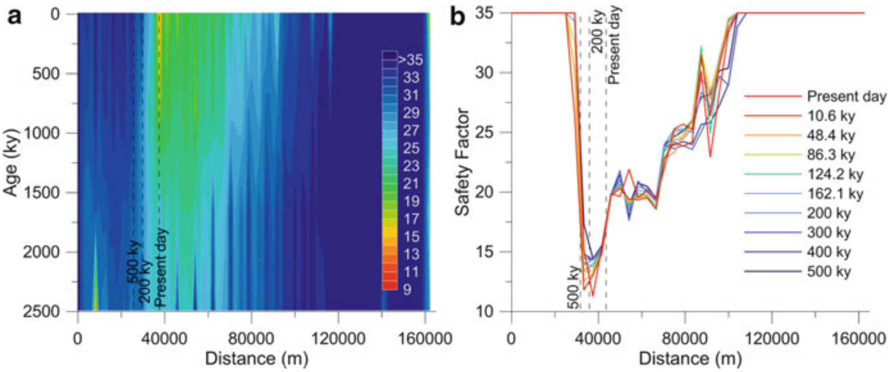

Fig. 9.5 (**a**) Evolution of the safety factor on the layer immediately below the seafloor. (**b**) Evolution of the safety factor on the R2 surface (∼0.5). *Dashed lines* represent the position of the shelf edge at different times during simulation

(layer immediately beneath) the FoS decreases with time in the slope area, but the lower values of FoS are still above 9. This fact shows that the slope has a higher control on the stability of the continental slope than overpressuring in the study area. At the maximum slope angle of 3º in the model, a minimum value of overpressure of 0.89 is needed for the slope to fail, highlighting that external mechanisms are needed to induce failure.

Weak layers are often involved in slope failure of Arctic and peri-Arctic regions (Vanneste et al. 2006). The high water content interglacial sediments that occur beneath rapidly deposited tills and GDFs can develop locally high overpressure zones which cannot be resolved in our model. Future work also needs to explore the effects of ice sheet erosion and isostatic compensation due to ice advance and retreat.

9.5 Conclusions

Consolidation tests of glacial and glacially influenced sediments of the upper slope of the Storfjorden TMF, western Barents Sea show that plumites (glacial melt-water plumites) have high void ratios, consolidation coefficients and permeabilities with respect to glacigenic debris flows at initial deposition conditions.

The compressibility and permeability values, together with stratigraphic input from seismic reflection profiles, were used in "BASIN" modeling. The modeling shows that onset of glacial sedimentation has a significant role in developing permeability barriers (tills) and/or allowing pore water drainage (GDFs). Occurrence of relatively uncompressible GDFs on the continental slope controls the margin fluid migration pathways.

Present day overpressure reaches a maximum value of 0.5 in the shelf area, 0.15 in the upper slope and 0.23 in the lower slope. These values of overpressure cannot trigger submarine landslides alone, but reduce the FoS of the margin by up to one half. Given the relatively reduced overpressure the FoS is mainly controlled by the evolution of the slope gradient during the margin development. An overpressure of more than 0.89 is needed to bring the FoS below 1. Also trigger mechanisms as glacio-eustatic rebound earthquakes can be considered.

Acknowledgements This study is funded by the "Ministerio Economia y Competitividad" through grants DEGLABAR, (CTM2010-17386), CORIBAR-ES (CTM2011-14807-E) and SVAIS (POL2006-07390). UNESCO and IUGS are also acknowledged for funding through project IGCP-585. The "Generalitat de Catalunya" is acknowledged for support through an excellence research group grant (2009-SGR-146). K. Andreassen and S. Clarke are thanked for their comments and positive criticism.

References

Bitzer K (1996) Modelling consolidation sedimentary and fluid basins flow. Comput Geosci 22:467–478

Bitzer K (1999) Two-dimensional simulation of clastic and carbonate sedimentation, consolidation, subsidence, fluid flow, heat flow and solute transport during the formation of sedimentary basins. Comput Geosci 25:431–447

Bugge T, Befring S, Belderson RH et al (1987) A giant three-stage submarine slide off Norway. Geo-Mar Lett 7:191–198

Butt FA, Elverhoi A, Solheim A et al (2000) Deciphering Late Cenozoic development of the western Svalbard Margin from ODP Site 986 results. Mar Geol 169:373–390. doi:10.1016/S0025-3227(00)00088-8

Dimakis P, Elverhoi A, Hoeg K et al (2000) Submarine slope stability on high-latitude glaciated Svalbard–Barents Sea margin. Mar Geol 162:303–316. doi:10.1016/S0025-3227(99)00076-6

Faleide JI, Solheim A, Fiedler A et al (1996) Late Cenozoic evolution of the western Barents Sea-Svalbard continental margin. Global Planet Change 12:53–74. doi:10.1016/0921-8181(95)00012-7

Flemings P, Long H, Dugan B et al (2008) Pore pressure penetrometers document high overpressure near the seafloor where multiple submarine landslides have occurred on the continental slope, offshore Louisiana, Gulf of Mexico. Earth Planet Sci Lett 269:309–325. doi:10.1016/j.epsl.2007.12.005

Haflidason H, Lien R, Sejrup HP et al (2005) The dating and morphometry of the Storegga Slide. Mar Petrol Geol 22:123–136. doi:10.1016/j.marpetgeo.2004.10.008

Karlsson R, Swedish Geotechnical Society, Laboratory Committee (1977) Consistency limits: a manual for the performance and interpretation of laboratory investigations. Statens rad for byggnads-forskning, Stockholm, pp 1–40

Knies J, Matthiessen J, Vogt C et al (2009) The Plio-Pleistocene glaciation of the Barents Sea–Svalbard region: a new model based on revised chronostratigraphy. Quat Sci Rev 28:812–829. doi:10.1016/j.quascirev.2008.12.002

Kvalstad TJ, Andresen L, Forsberg CF et al (2005) The Storegga slide: evaluation of triggering sources and slide mechanics. Mar Petrol Geol 22:245–256. doi:10.1016/j.marpetgeo.2004.10.019

Laberg J, Vorren T, Dowdeswell J et al (2000) The Andøya Slide and the Andøya Canyon, north-eastern Norwegian–Greenland Sea. Mar Geol 162:259–275. doi:10.1016/S0025-3227(99)00087-0

Laberg JS, Vorren TO, Mienert J et al (2002) Late Quaternary palaeoenvironment and chronology in the Trænadjupet Slide area offhore Norway. Mar Geol 188:35–60

Laberg JS, Andreassen K, Knies J et al (2010) Late Pliocene-Pleistocene development of the Barents Sea ice sheet. Geology 38:107–110. doi:10.1130/G30193.1

Lucchi RG, Pedrosa MT, Camerlenghi A et al (2012) Recent submarine landslides on the continental slope of Storfjorden and Kveitehola Trough – Mouth Fans (NW Barents Sea). In: Yamada Y et al (eds) Submarine mass movements and their consequences, vol 31, Advances in natural and technological hazards research., pp 735–745. doi:10.1007/978-94-007-2162-3

Mulder T, Moran K (1995) Relationship among submarine instabilities, sea level variations, and the presence of an ice sheet on the continental shelf: an example from the Verrill Canyon Area, Scotia Shelf. Paleoceanography 10:137–154

Rebesco M, Pedrosa MT, Camerlenghi A et al (2012) One million years of climatic generated landslide events on the northwestern Barents Sea continental margin. In: Yamada Y et al (eds) Submarine mass movements and their consequences, vol 31, Advances in natural and technological hazards research. Springer, Dordrecht, pp 747–756

Shaver RB (1998) The determination of glacial till specific storage in North Dakota. Ground Water 32:552–557

Urgeles R, Locat J, Sawyer DE et al (2010) History of pore pressure build up and slope instability in mud-dominated sediments of Ursa Basin, Gulf of Mexico continental slope. In: Mosher DC (ed) Submarine mass movements and their consequences, vol 28, Advances in natural and technological hazards research. Springer, Dordrecht, pp 179–190

Van Hinte JE (1978) Geohistory analysis; application of micropaleontology in exploration geology. AAPG Bull 62:201–222

Vanneste M, Mienert J, Bunz S (2006) The Hinlopen Slide: a giant, submarine slope failure on the northern Svalbard margin, Arctic Ocean. Earth Planet Sci Lett 245:373–388. doi:10.1016/j.epsl.2006.02.045